SUPPLEMENTARY METHODS

Splenocyte isolation

Three to five C3aR1 knockout (Jackson Laboratory, C.129S4-C3ar1tm1Cge/J, stock number 005712) and specific wt BALB/cJ mice were euthanized with CO_2 and spleens were harvested. Spleens were placed in complete media (RMPI with 10% FBS, 1% 2-mercaptoethanol and 1% penicillin/streptomycin) and filtered through a 100µm, then 70µm mesh nylon screen to yield a single-cell suspension. Red blood cells were removed with 5ml of ACK lysis buffer (150mM NH4Cl, 10mM $KHCO_3$, 0.1mM Na_2EDTA, pH 7.4) and incubated for 5 minutes. 10ml of complete media was added to wash cells; cells were centrifuged (10min at 200x g) and supernatant was discarded. The splenocytes were washed two additional times with complete media. Splenocytes were seeded at $1x10^6$ cells/ml and stored in an incubator (37°C, 5% CO_2) for 4 hours until NMR sample preparation. All animal experiments were approved by the IACUC, University of Minnesota.

Gastric contraction assay

Wistar female rats (250-350 g; Charles River) were euthanized by inhalation of 75% CO_2 in air. The stomach was removed and washed in fresh Tyrode's solution as previously described (Severini et al., 2009). Longitudinal strips were obtained from the rat longitudinal forestomach (RLF) musculature and mounted vertically in a 5 ml organ bath in oxygenated (95% O_2 and 5% CO_2) Tyrode's solution at 37 °C. Responses were recorded isotonically by a strain gauge transducer (DY 1, Basile, Milan, Italy) and displayed on a recording microdynamometer (Unirecord, Basile. Milano, Italy). Tissues were allowed to equilibrate for about 60 min and the superfusion buffer was changed every 10 min. Saturating concentrations of acetylcholine (ACh, 25 µM) were added every 20 min, washing the tissue after 1 min contact time, until reproducible contractile responses were obtained. After 30 min equilibration time, peptide activity was tested,

washing the tissue as soon as the contraction peak had developed, after a contact time with muscle strips of 1-3 min. Since we demonstrated that an interval of 20 min was necessary to obtain a complete recovery, this interval was used for every peptide addition. Peptides were purchased from Primm (Milano, IT) C3a70-77 for Anaspec (USA) and C3aR1 antagonist from Calbiochem (USA). Data were analyzed with unpaired t-tests. All animal experiments were approved by the Ethics Committee of the Italian Ministry of Health.

GPCR β-arrestin recruitment assay: G-protein independent

The assay was done as previously reported (Lin et al., 2013). Briefly, HTLA cells (an HEK293 cell line stably expressing a tTA-dependent luciferase reporter and a β-arrestin2-TEV fusion gene) were cultured in DMEM supplemented with 10% FBS and 5 µg/ml. Puromycin and 100 µg/ml Hygromycin. HTLA cells were transfected with C3aR-tTA construct using the calcium phosphate method and incubated overnight at 37°C. Cells were plated in Poly-L-Lys (PLL) coated 384-well white clear bottom cell culture plates at a density of 15,000 cells in 50 µl per well of DMEM with 1% dFBS and incubated overnight. Drug solutions were prepared in sterile 1XHBSS, 20 mM HEPES, pH 7.4 (assay buffer) at 6x dilution and added to cells (10 µl per well) for overnight incubation at 37°C. The following day, the medium was replaced by 20 µl per well of BrightGlo reagent (diluted 10-x with assay buffer). Plates were incubated for 20 minutes at room temperature in the dark before being counted on a luminescence counter.

SUPPLEMENTAL FIGURE LEGENDS

Figure S1, related to Figure 1 and Figure S4. Gene expression of C3ar1. C3aR1 mRNA was measured by real time QPCR in 3T3L1, N38 and CHO cells and normalized over β-actin expression.

Figure S2, related to Figure 2. Software prediction and secondary structural characterization of free TLQP-21. **A**) Two dimensional total correlation spectroscopy spectrum of TLQP-21 dissolved in NMR buffer at acquired at 37ºC. Only the amide region (~7-9ppm) is shown for clarity. **B**) Secondary structural prediction of TLQP-21 using JUFO and PredictProtein software. **C**) Chemical Shift index ($\Delta H\alpha$) of TLQP-21 using assigned $H\alpha$ chemical shift in (**A**). **D**) Overlay of TLQP-21 rINEPT in the absence (black) and presence (red) of small unilamellar vesicles composed of DOPC/DOPE lipids. No changes in chemical shift are detected when TLQP21 interacts with SUVs. Asterisks indicate natural abundance 13C of lipid molecules.

Figure S3, related to Figure 2. TLQP-21 peptide synthesis and chemical characterization. **TOBSY and INEPT spectra. A**) Sequences of TLQP21 mouse isoform with the location of isotopic labeling. **B**) Overlay of two 15N-HSQC fingerprinting spectra of TLQ-P21 corresponding to the isotopic labeled peptides (blue = ALP labeling, red=PARRPA labeling). **C**) SDS-PAGE of purified synthetic TLQP21 stained with Coomassie. **D**) Analytical HPLC trace showing single peak corresponding to pure TLQP-21. **E**) TOBSY and INEPT spectra of $^{13}C/^{15}N$ TLQP-21 (P4-A6-R9) in buffer (red) or in presence of 3T3L1 cells (blue) illustrating the assignment of the resonances. INEPT spectrum contains only signals from 13C-1H pairs. TOBSY spectrum contains the signals from the adjacent ^{13}C-^{13}C groups, allowing for the spin system assignment.

Figure S4, related to Figure 4. **Structural analysis of TLQP-21 in presence of N38 cells.** Refocused INEPT spectra of TLQP-21, labeled with ^{13}C and ^{15}N at A_{16}-L_{17}-P_{18} with resonance assignments indicated. Experiments were performed in buffer (**A**), in the presence of 3T3L1 cells (**B**) or in the presence of N38 cells (**C**).

Figure S5, related to Table 1. Gastric fundus strip contraction assay. **A**) Graphs shows example of the contractile responses evoked by TLQP-21 (top arrows) and the C-terminal mutants P18A, P19A and R21A. **B**) The C3a71-77 induces a contraction similar to TLQP-21 while the C3aR1 antagonist SB290157 antagonizes TLQP-21-induced contraction of stomach fundus strips. *p>0.5, **<0.01, **<0.001.

Figure S6, related to Figure 5. A) Isoproterenol but not TLQP-21 dose-dependently increases lipolysis in 3T3L1 adipocytes ($F(3, 45)=58.2$, $p=.000001$). **B**) TLQP-21 dose-dependently increases lipolysis induced by 50nM isoproterenol ($F(5, 38)=101.8$, $p<0.00001$). The most effective dose of TLQP-21 is 100nM after which a plateau is reached. TLQP-21 100nM does not increase lipolysis in absence of isoproterenol. **C**) Unlike TLQP-21 (Possenti et al., 2012), the R21A mutant peptide does not potentiate isoproterenol-induced AMPK phosphorylation in 3T3L1 adipocytes. # p<0.06, *p<0.05, **p<0.01 vs control.

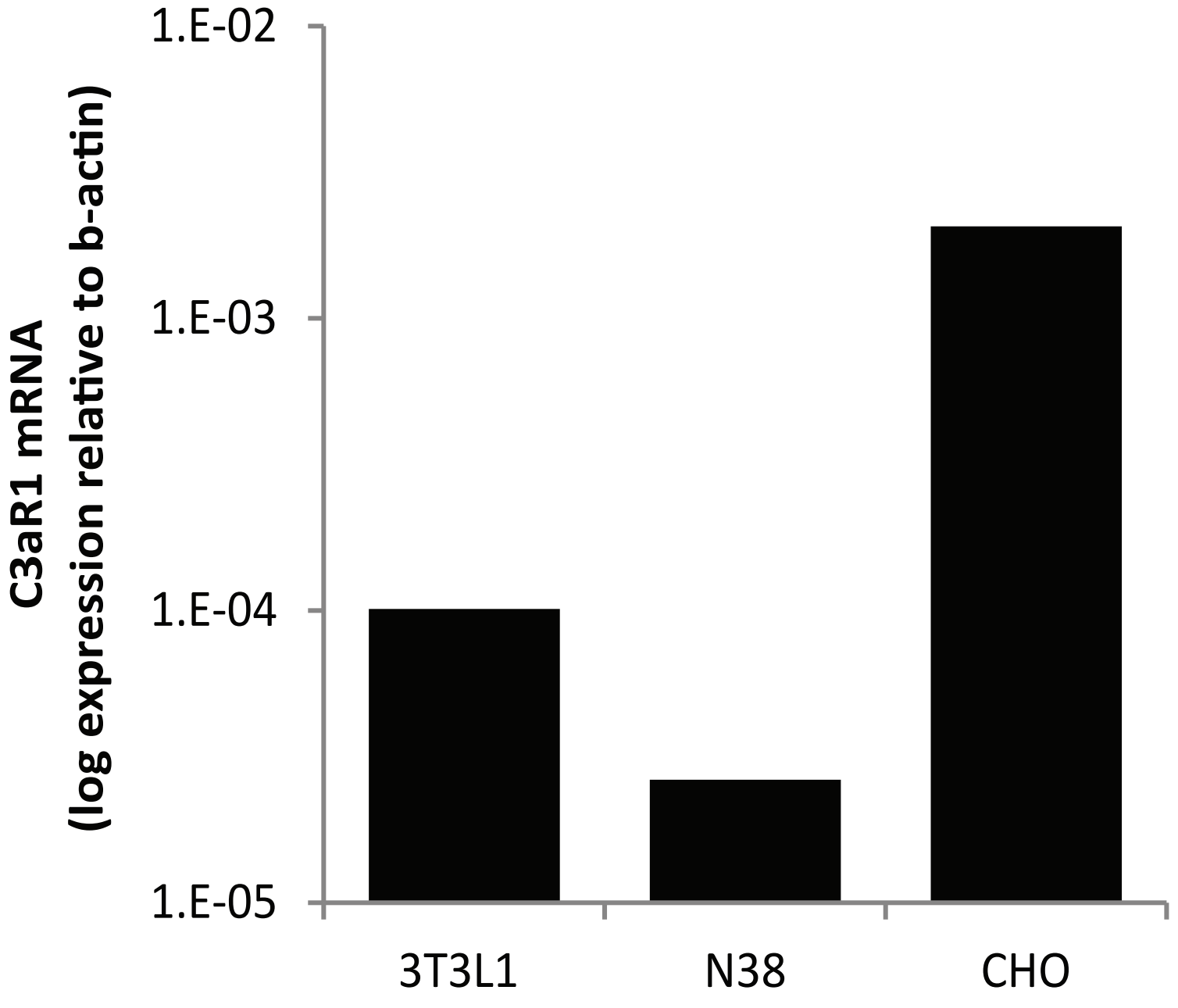
C3aR1 mRNA
(log expression relative to b-actin)
1.E-02
1.E-03
1.E-04
1.E-05
3T3L1
N38
CHO

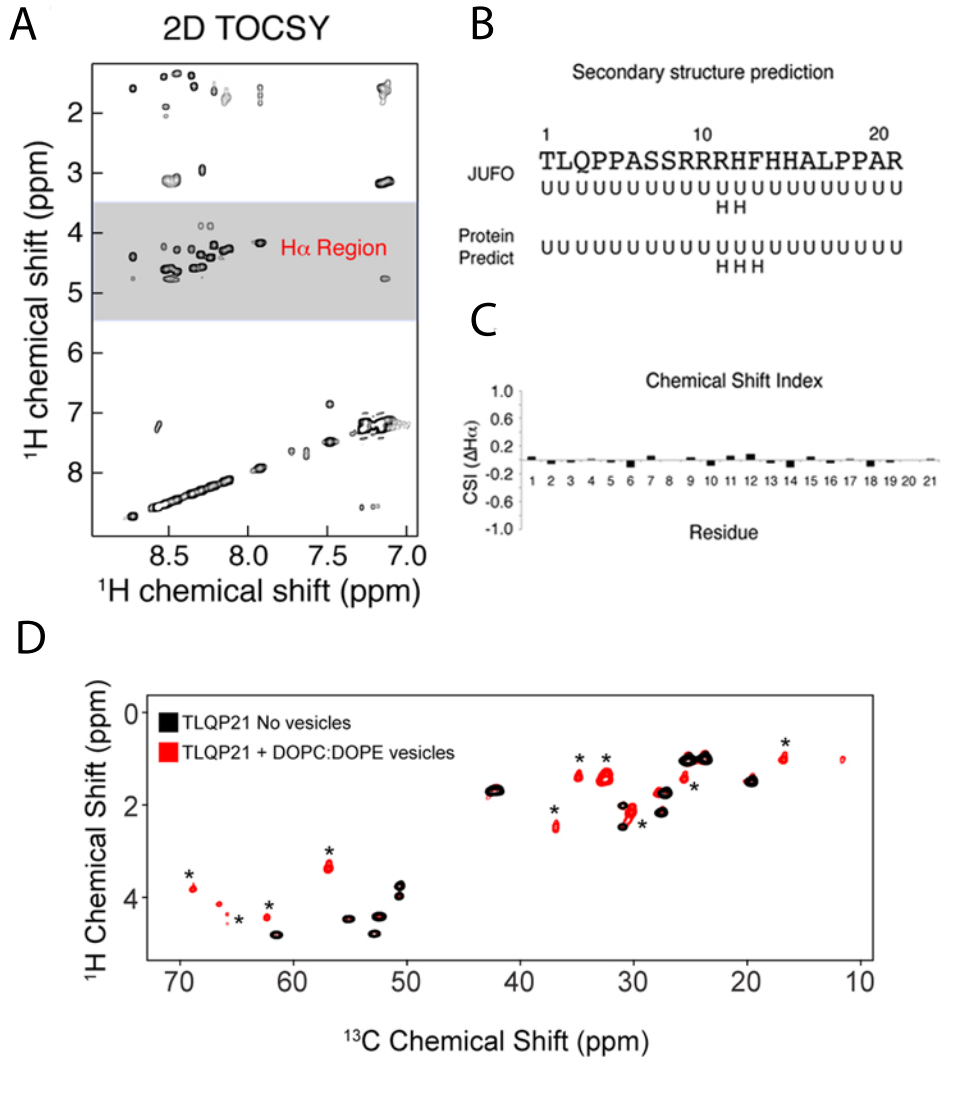
A
2D TOCSY
Hα Region
¹H chemical shift (ppm)
¹H chemical shift (ppm)
B
Secondary structure prediction
1
10
20
JUFO
TLQPPASSRRRHFHHALPPAR
H H
Protein Predict
H H H
C
Chemical Shift Index
CSI (ΔHα)
Residue
D
TLQP21 No vesicles
TLQP21 + DOPC:DOPE vesicles
¹H Chemical Shift (ppm)
¹³C Chemical Shift (ppm)

A

TLQPPASSRRRHFHHALPPAR

TLQPPASSRRRHFHH(^{15}N-^{13}C-ALP)PAR

TLQ(^{15}N-^{13}C-P)P(^{15}N-^{13}C-A)SS(^{15}N-^{13}C-R)R(^{15}N-^{13}C-R)HFHHALP(^{15}N-^{13}C-P)(^{15}N-^{13}C-A)R

B

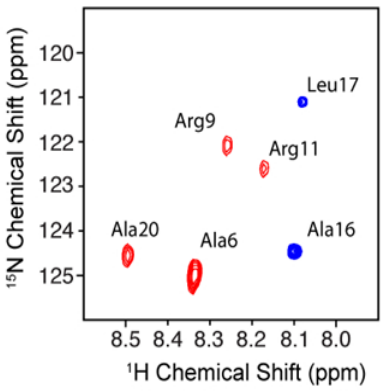

C

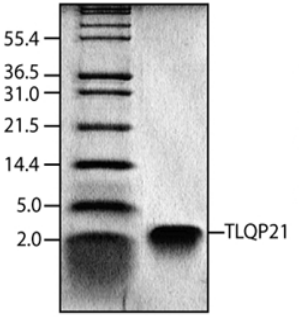

D

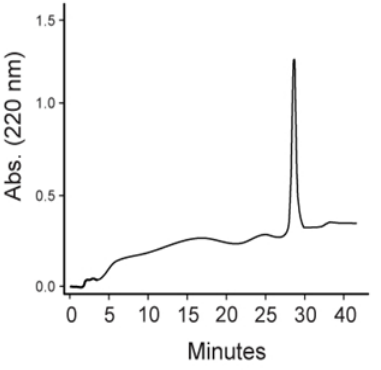

E

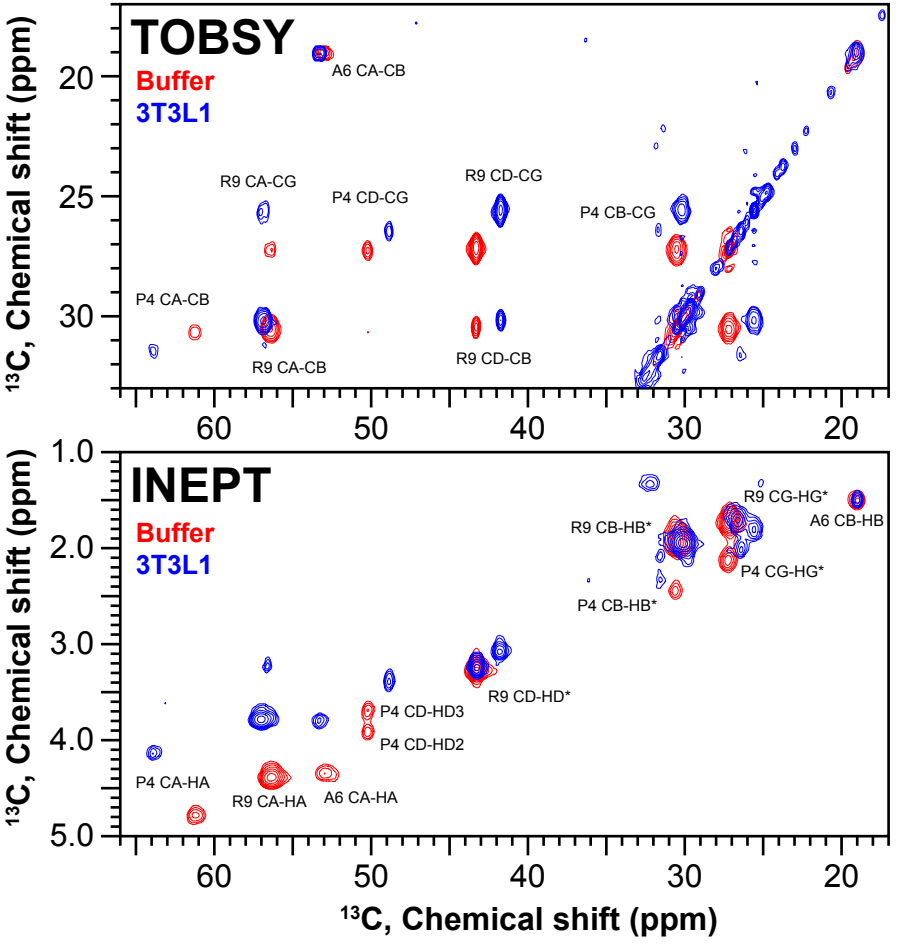

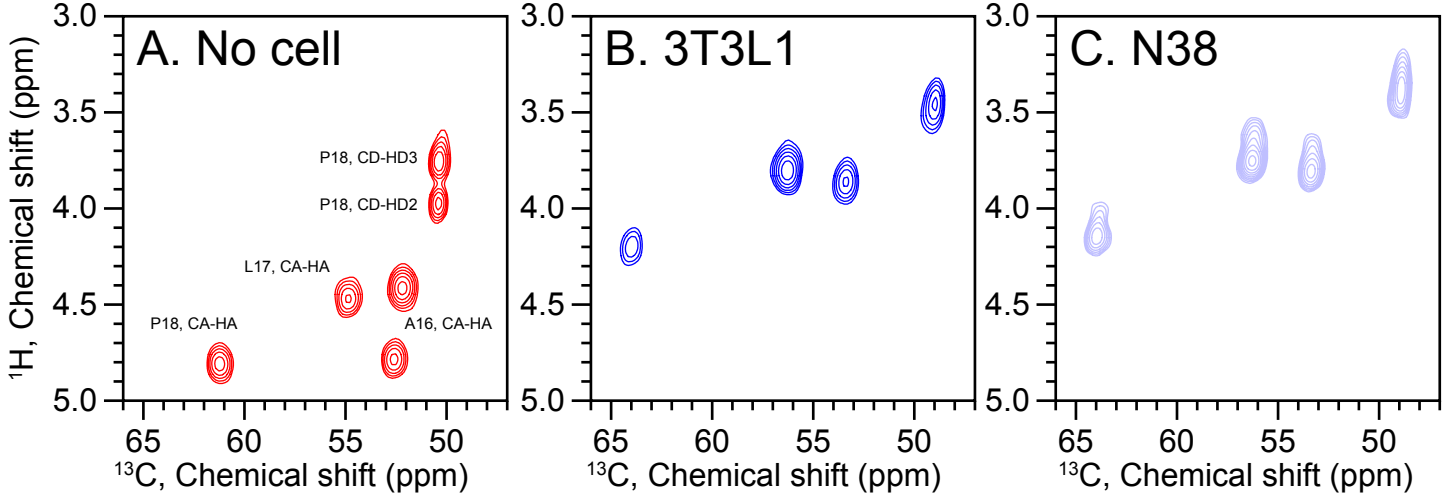
A. No cell
B. 3T3L1
C. N38
P18, CD-HD3
P18, CD-HD2
L17, CA-HA
P18, CA-HA
A16, CA-HA
^{1}H, Chemical shift (ppm)
^{13}C, Chemical shift (ppm)
3.0
3.5
4.0
4.5
5.0
65
60
55
50

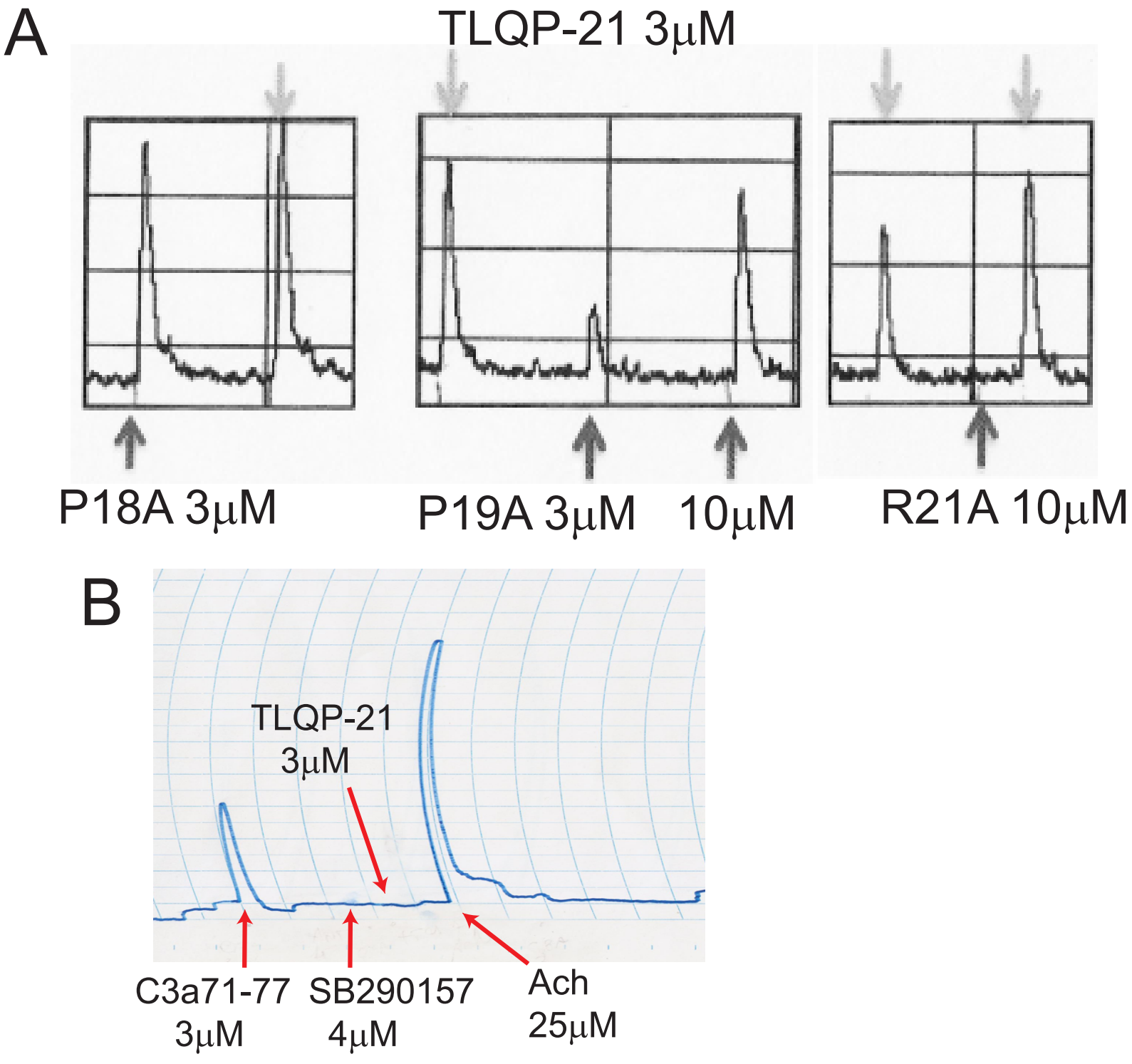
A
TLQP-21 3μM
P18A 3μM
P19A 3μM
10μM
R21A 10μM
B
TLQP-21
3μM
C3a71-77
3μM
SB290157
4μM
Ach
25μM

A

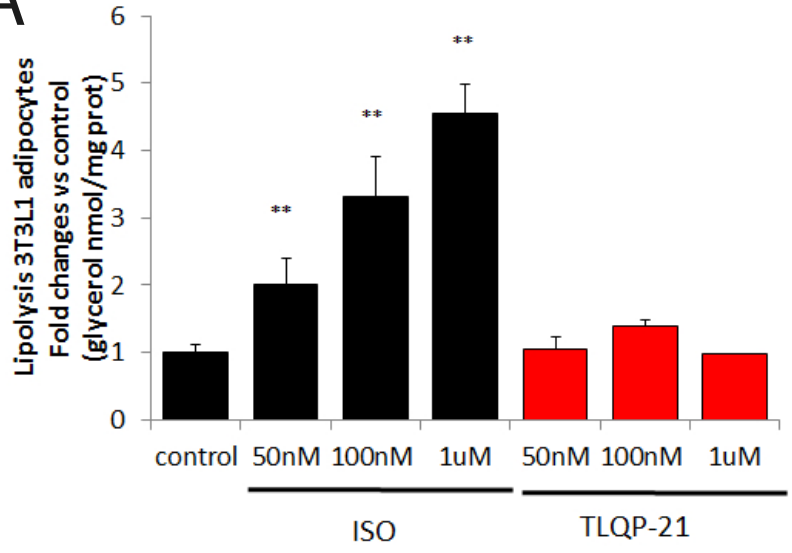
Lipolysis 3T3L1 adipocytes
Fold changes vs control
(glycerol nmol/mg prot)
0
1
2
3
4
5
6
**
**
**
control
50nM
100nM
1uM
50nM
100nM
1uM
ISO
TLQP-21

B

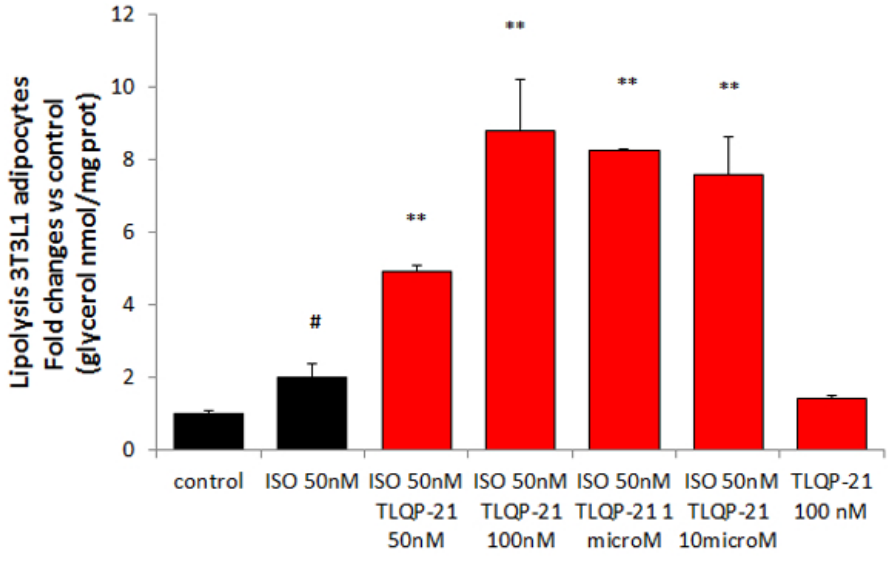
Lipolysis 3T3L1 adipocytes
Fold changes vs control
(glycerol nmol/mg prot)
0
2
4
6
8
10
12
#
**
**
**
**
control
ISO 50nM
ISO 50nM TLQP-21 50nM
ISO 50nM TLQP-21 100nM
ISO 50nM TLQP-21 1 microM
ISO 50nM TLQP-21 10microM
TLQP-21 100 nM

C

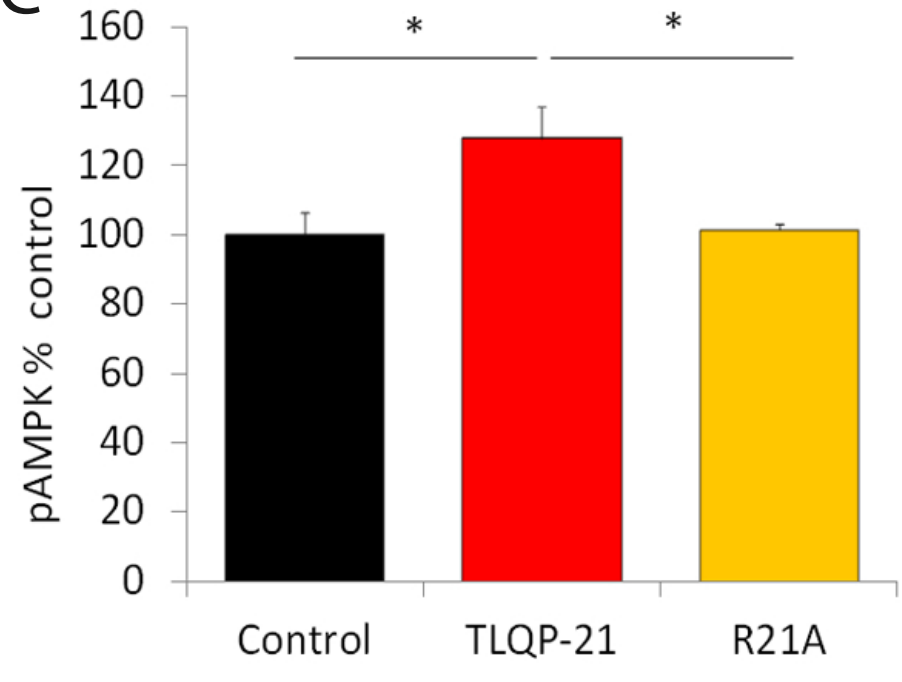
pAMPK % control
0
20
40
60
80
100
120
140
160
*
*
Control
TLQP-21
R21A